Analytical Methods

ROYAL SOCIETY OF CHEMISTRY

PAPER

View Article Online
View Journal | View Issue

Cite this: *Anal. Methods*, 2021, **13**, 719

The development of an electrochemical DNA biosensor based on quercetin as a new electroactive indicator for DNA hybridization detection

Esmaeel Alipour, * Sheida Norouzi and Shokoufeh Moradi

Received 26th October 2020
Accepted 24th December 2020

DOI: 10.1039/d0ay01993c

rsc.li/methods

An electrochemical DNA biosensor was designed for the detection of a specific target DNA after hybridization with a complementary DNA probe immobilized onto a glassy carbon electrode surface. Quercetin was successfully used as a new electroactive indicator for the hybridization detection. Different interactions of quercetin with single-stranded DNA (ss-DNA) and double-stranded DNA (ds-DNA) led to different electrochemical signals, which were recorded as cyclic and differential pulse voltammograms enabling hybridization detection. Various parameters influencing the biosensor performance were evaluated, and optimized conditions were obtained. Also, the detection limit of 83 pM with a relative standard deviation of 4.6% was obtained for the determination of complementary oligonucleotides. Then, the developed biosensor was applied successively for the detection of short sequences of hepatitis C virus (HCV1). The hybridization between the probe (PHCV1) and its complementary sequence (HCV1a) as the target was studied. Some hybridization experiments with noncomplementary oligonucleotides also showed that the suggested DNA sensor responds selectively to the target.

1. Introduction

Molecular diagnosis is the process of identifying a disease by studying molecules, such as proteins, DNA and RNA in a tissue or fluid, which expanded rapidly in the past decade, offering a sensitive, inexpensive and quantitative method for the analysis of genomic sequences in order to detect diseases and gene mutations. DNA hybridization is one of the most widely used methods, and is the process in which two or more complementary strands of DNA are coiled around each other. The basis of this event is the setting of these bases in front of each other.[1]

A biosensor is an analytical tool for DNA hybridization detection that consists of a biological part in combination with a transducer. The role of the transducer is to convert the recognized biological event into a measurable signal, such as an electrochemical signal like current.[2] Among all sensors, electrochemical biosensors or electrochemical transducers hold a specific position due to the high sensitivity, ease of work and handling, small dimensions, ease of immobilization of DNA layer and *etc.*[3] The basis of detection is measuring current changes due to the hybridization of the DNA probe with strands that contain its complementary bases under a controlled potential. Probes used in biosensors are usually oligonucleotides with 15–50 bases in their structures. The amount of immobilized probe and hybridization time (probe and target DNA strands should have enough freedom to twist around each other) determine the selectivity, sensitivity and reproducibility. Different methods have been reported for the electrochemical detection of hybridization, and are classified into two categories. The first category includes methods that are based on the intrinsic electrochemical properties of DNA; for example, the detection of the oxidation current of guanine or adenine bases.[4] However, in the second category, the electrochemical signal changes related to electroactive indicators are monitored after hybridization. Also, the two mentioned groups are denominated as label-free or label-based methods. In other words, as described earlier, in the label-free methods, the electrochemical signal is only due to the hybridization event and only the target DNA is responsible for it. It seems that the direct or label-free detection methods are simple, but they are not more sensitive.[5]

Investigations on the label-free DNA hybridization methods are not as common as that for the label-based methods. In 1998, Wang *et al.*[6] developed an electrochemical biosensor for the direct recognition of DNA hybridization without using any redox indicator. Pournaghi-azar and co-workers[7] also reported a number of works on DNA biosensors based on direct hybridization detection. For more information, readers are referred to ref. [8–11]. In the label-based methods, the obtained electrochemical signal defines the extent of interaction between

Electroanalytical Chemistry Laboratory, Department of Analytical Chemistry, Faculty of Chemistry, University of Tabriz, Tabriz, Iran. E-mail: i-alipour@tabrizu.ac.ir; Fax: +98 413 3340191; Tel: +98 413 3340191

the redox indicator molecules and ss-DNA or ds-DNA. As a whole, small molecules bind to DNA *via* mechanisms, such as electrostatic interaction, intercalation between base pairs and minor or major DNA grooves binding interaction.[12] DNA is the pharmacological target of many of the drugs that are currently in clinical use or in advanced clinical trials. So, the study of the interaction of drug and DNA is of great significance for designing and synthesizing the new drugs targeted to DNA, and their effectiveness depends on the mode and affinity of the binding.[13] Some papers on the interaction between DNA and different drugs are presented by Hossieny Ibrahim.[12–16] On the other hand, the development of biosensors for hybridization detection using electroactive redox indicators opened a way for the most exciting discoveries because of their high sensitivities and low detection limits. These redox indicators differentiate between ss-DNA and ds-DNA, while their affinity to ds-DNA is usually more than ss-DNA. Many studies have been conducted on label-based methods. In 1998, Erdem and co-workers[17] reported the use of $Co(Phen)_3^{3+}$ as a redox hybridization indicator. In 2002, Yang *et al.*[18] used Methylene blue as an electroactive indicator for DNA hybridization detection. In 2006, Pournaghi-azar and his co-workers[19] developed an electrochemical DNA biosensor using pencil lead as a working electrode and Methylene blue as an electrochemical indicator. In 2010, Gao *et al.*[20] successfully used Toluidin blue as a new electroactive hybridization indicator. Additional papers published on label-based DNA hybridization biosensors are in ref. [21–25].

Quercetin is a flavonoid compound, which has attracted much attention because of its biological and pharmaceutical specificity. It is present in plants, such as tea, onion, and apple. Because of the polyphenolic structure, it is an anti-oxidant and radical scavenger. Many research studies show that quercetin has beneficial effects on health too. There are not many reports on the electrochemical investigation of flavonoids. Quercetin has 5 hydroxyl groups that are electroactive, and so it can be oxidized or reduced, while the oxidation is pH dependent. Regardless, many electroactive DNA hybridization indicators with high sensitivity have been introduced up to now. Because of their toxicity, they cannot be used for *in vivo* research studies. As mentioned earlier, quercetin is a non-toxic flavonoid and also has anti-oxidation and anti-cancer properties.[26–29] The aim of this work is the detection of a DNA hybridization event using a simple electrochemical method, and so the capability of quercetin as a new DNA hybridization redox indicator was investigated. The electrochemical behavior of quercetin as a redox hybridization indicator was studied on a DNA-modified glassy carbon electrode (GCE) using differential pulse voltammetry (DPV) and cyclic voltammetry (CV). The developed biosensor was applied successfully for the detection of short sequences of the hepatitis C virus (HCV1) as a model.

2. Materials and methods

2.1. Reagents

All of the oligonucleotides were supplied as a lyophilized powder from MWG-Biotech Company and or from Denazist Company (mashhad-Iran), and their sequences are listed in Table 1. The stock solutions (100 μM) of the oligonucleotides were prepared with distilled water, while for further diluted solutions, Tris chloride at 0.01 M (pH = 7) buffer containing 30 mM NaCl was used. All of the prepared solutions were stored in a freezer at −24 °C. The preparation of quercetin solutions was done in two ways. In the first way, a defined amount of quercetin was dissolved in NaOH solution with a final concentration of 100 μM. In the other way, ethanol (purity, 95%) was used as a solvent. The concentration of quercetin was 1 mM. Tris buffer at 0.01 M (pH = 7.01) was prepared and used for providing DNA solutions. Also, acetate buffer at 0.5 M (pH = 4.8) was used as a background buffer. Deionized water was used for all solutions. In addition, all containers, glassware and sampler tips were sterilized by autoclave.

2.2. Apparatus

All experiments were performed by autolab (PGSTAT30, Netherlands) using GPES (4.9 version) software as a data recorder. A three-electrode system consisted of an Ag/AgCl reference electrode, glassy carbon working electrode (2 mm diameter) and a platinum counter electrode. All of the electrodes were purchased from Azar electrode, Iran. A magnetic vortex (model 649, Metrohm, Switzerland) was used for stirring solutions and creating permanent conditions for the probe immobilization and washing of the electrode surface.

2.3. Procedure

In order to remove the contaminants and produce a smooth surface for all experiments, the GCE surface was polished with alumina and cleaned with an ultrasonic cleaner containing distilled water for 5 min. All of the experiments were done at room temperature without expelling the oxygen of solutions.

2.3.1. Probe immobilization onto GCE. The prepared working electrode was immersed in a solution of Tris chloride buffer at 0.01 M (pH = 7.01) that contains the DNA probe at 5 μM (poly A) and NaCl at 30 mM, while a constant potential of −0.5 V was applied for 300 s. Then, the electrode (poly A modified – GCE) was rinsed by distilled water using a magnetic stirrer.

2.3.2. Hybridization on the poly A modified – GCE. The poly A modified – GCE was put in Tris–HCl buffer at 0.01 M (pH = 7.01) solution containing 5 μM poly T and 30 mM NaCl (hybridization buffer solution), and then a potential of 0.5 V was applied for 300 s. Subsequently, the electrode was rinsed with stirred distilled water for 2 min. In the same way, the probe-modified electrode was immersed in the solution of the non-complementary oligonucleotide.

2.3.3. Accumulation of quercetin on the probe-modified electrode. Bare or poly A modified – GCE before and or after hybridization was mounted into a 0.35 M acetate buffer (pH = 4.8) solution containing 50 μM quercetin and 83 mM NaCl. Then, it was stirred for 5 min and the electrode was rinsed by stirring distilled water for 2 min.

2.3.4. Voltammetric measurements. Cyclic voltammetry and differential pulse voltammetry were used for studying the events happening at the electrode surface. For CV studies, poly A modified – GCE was immersed into the 0.35 M acetate

Table 1 Oligonucleotide sequences

Oligonucleotide	Supplied from	Sequence
Poly A	Denazist Company	5′-AAA AAAAAAAAAAAAAA-3′
Poly T	Denazist Company	5′-TTT TTTTTTTTTTTTTT-3′
Poly C	Denazist Company	5′-CCC CCCCCCCCCCCCCC-3′
Poly G	Denazist Company	5′-GGG GGGGGGGGGGGGG-3′
PHCV1 (probe)	MWG-Biotech Company	5′-CCCACCCGCAGCCCTCATTA-3′
HCV1a (complementary)	MWG-Biotech Company	5′-TAATGAGGGCTGCGGGTGGG-3′
HCV3a (non-complementary)	MWG-Biotech Company	5′-GTGGGTGATATGTGTGG-3′

solution (pH = 4.8) containing 83 mM NaCl and 86 mM quercetin, while the sweeping potentials in the range of (0.0–0.55) V were applied with different scan rates. For DPV studies, the provided electrode was mounted in the 0.35 M acetate solution (pH = 4.8) containing 83 mM NaCl, and the potential was applied in the range of (0.0–0.6) V using a pulse amplitude of 25 mV.

3. Results and discussion

3.1. Electrochemical behavior of quercetin

The effect of different scan rates were studied because of two purposes: first, the determination of the nature of the oxidation current of quercetin (if it is due to diffusion or adsorption), and the second is the comparison of the electrochemical behavior of quercetin on bare and DNA modified – GCE surface. Fig. 1 shows the cyclic voltammograms of the bare (Fig. 1A) and DNA modified GCE (Fig. 1B), respectively, in acetate buffer solution containing 86 μM quercetin. As shown in Fig. 1A and B, the anodic peak currents of quercetin were increased by scan rates using the bare and DNA-modified GCE, respectively. Also, the changes of the oxidation peak current of quercetin *versus* the scan rate and square root of the scan rate were shown as inset diagrams in Fig. 1. Linear changes of the current in terms of the scan rate with a correlation coefficient of 0.997 (Fig. 1A, inset x) show that the oxidation of quercetin on the bare GCE surface is diffusive, while the correlation coefficient of 0.994 in (Fig. 1B, inset y) implies that the oxidation of quercetin on the DNA-modified GCE surface is under the control of adsorption.

Fig. 2 shows the Tafel plot derived from the rising part of the voltammograms b shown in Fig. 1A and B. The related Tafel curves are seen in the inset.

According to the method of Nicholson,[30] the heterogeneous rate constants of the electron transfer (k°) were calculated from the cyclic voltammetry peak-to-peak separation, (ΔE_p), by using the numerically evaluated relationship between ΔE_p and the ψ function.

$$\psi = \left(\frac{RT}{nFD\pi\nu}\right)^{1/2} k^\circ$$

By assuming $n_\alpha = 1$, the obtained α values for the electro-oxidation of quercetin on the bare and poly A modified – GCE are 0.42 and 0.45, respectively.

So, first the $n\Delta E_p$ was obtained from the corresponding cyclic voltammograms in several potential scan rates (Fig. 1A and B, for scan rates of 5, 10, 25 and 50 mV s^{-1}). In addition, using the Nicholson working curve, the ψ values were determined for the mentioned scan rates. Then, the plot of ψ *versus* the $\nu^{-1/2}$ was obtained (Fig. 3).

By considering the slope of this plot and also assuming that $D = 10^{-5}$ cm^2 s^{-1} for quercetin and $n = 2$, the values of k° for the bare GCE and DNA-modified GCE were calculated to be 0.135 and 0.156 cm s^{-1}, respectively.

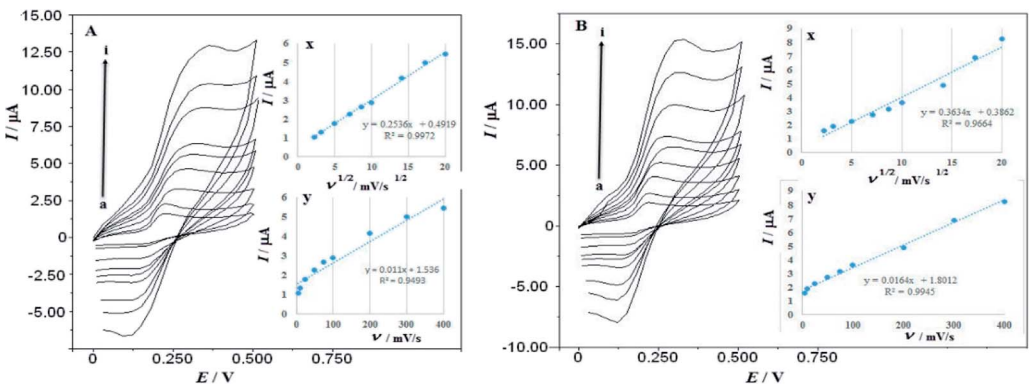

Fig. 1 CVs of the bare GCE (A) and poly A modified – GCE (B) in 0.35 M acetate buffer solution (pH = 4.8) containing 86 μM quercetin and 83 mM NaCl at scan rates of (inner to outer): 5, 10, 25, 50, 75, 100, 200, 300, 400 mV s^{-1}. Inset x: The plot of the peak current *vs.* the square root of the scan rate ($\nu^{1/2}$). Inset y: The plot of the peak current *vs.* scan rate (ν). Experimental conditions: poly A modified – GCE was prepared as described in Section 2.3.1.

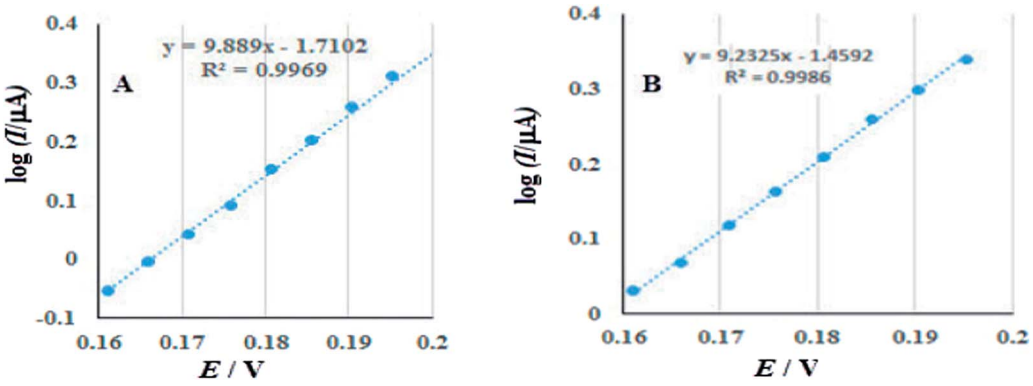

Fig. 2 Tafel plot derived from the rising part of the voltammograms b shown in Fig. 1A and B.

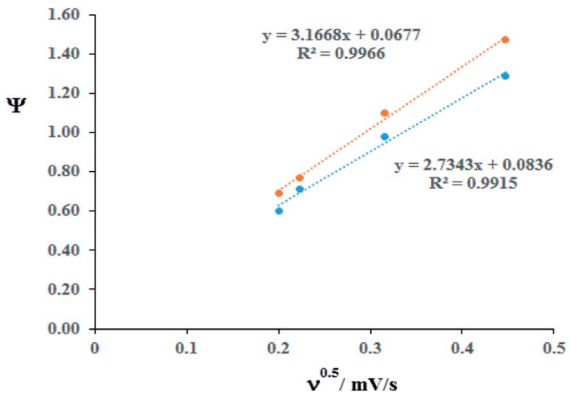

Fig. 3 Plot of ψ *versus* the $\nu^{-1/2}$.

3.2. Characterization of the DNA-modified GCE

3.2.1. EDX mapping analysis. A DNA molecule comprises nucleotide units, and each of these nucleotides is composed of one of four nitrogen-containing nucleobases (adenine, guanine, cytosine or thymine), a phosphate group and a sugar called deoxyribose. The spatial distributions of the atomic contents (N, P, C and O) across the DNA-modified GCE surface was obtained using energy dispersive X-ray spectroscopy (EDX) analysis (Fig. 4), which confirms the presence of P, C, N and O atoms, indicating that the surface of the GCE was successfully modified with DNA oligonucleotides.

3.2.2. Electrochemical impedance spectroscopy (EIS) study. The electrochemical impedance spectroscopy was carried out using a potentiostat-galvanostat (Origalys, Origa Flex 01A, France) at the 100 kHz–100 mHz frequency range with ±10 mV AC voltage at an open circuit potential (OCP). A conventional three-electrode cell equipped with a Pt plate (as a counter electrode), saturated calomel (SCE, as reference electrode), and GC-coated DNA (as the working electrode) was employed in these experiments. The 10 mM $[Fe(CN)_6]^{4-/3-}$ solution containing KCl (0.1 M) was used as an electrolyte. The EIS results were fitted with Z view II software. The Nyquist plots of the bare GCE, ss-DNA modified GCE and ds-DNA modified GCE are illustrated in Fig. 5.

The one semicircle equivalent circuit model along with a Warburg element was used for fitting the EIS results (Fig. 6). In this model, R_s is the electrolyte resistance, CPE is the constant phase element of the electrical double layer, R_{ct} is the charge

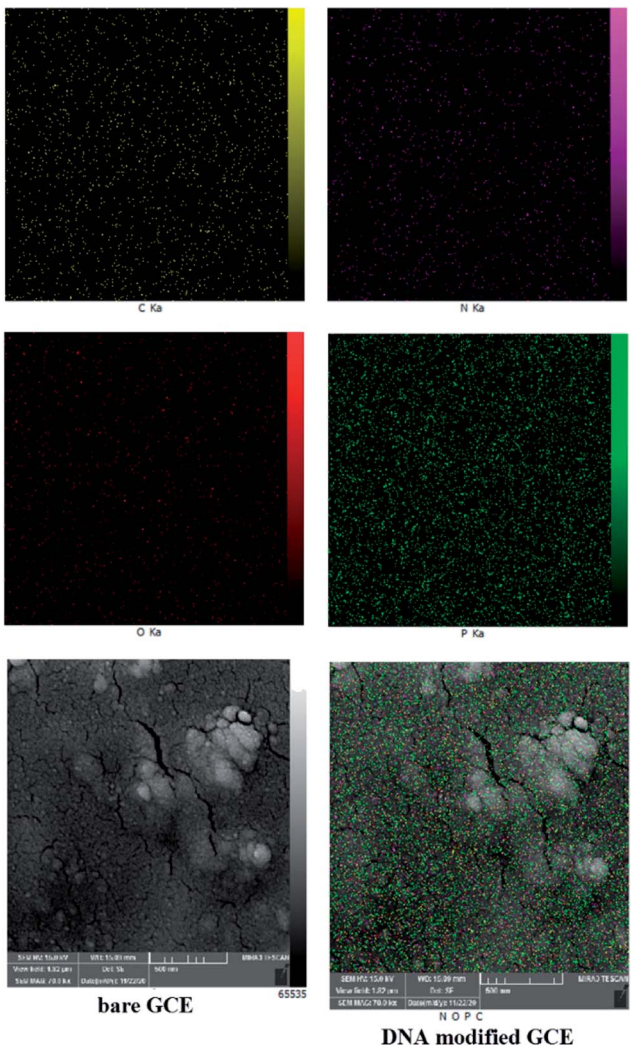

Fig. 4 Energy dispersive X-ray (EDX) mapping analysis of the bare and DNA-modified GCE.

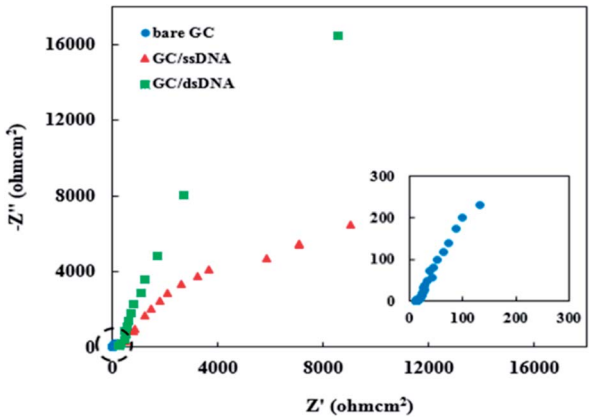

Fig. 5 Nyquist plots of the bare GCE, ss-DNA and ds-DNA modified GCE in the 10 mM $[Fe(CN)_6]^{4-/3-}$ solution containing 0.1 M KCl.

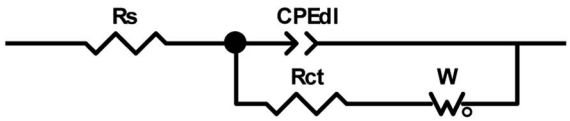

Fig. 6 Equivalent circuit model for fitting EIS data.

transfer resistance, and W is the Warburg element at low frequencies.

The extracted EIS parameters are presented in Table 2.

It can be seen that the R_{ct} of the ds-DNA modified GCE is 1.54 and 33.69 times higher than that for the ss-DNA modified and bare GCE, respectively. The interfacial charge transfer resistance of the ss-DNA modified GCE is higher than that for the bare GCE. The reason for this increase was that the surface of the ss-DNA modified GCE has a negative charge that prevented $[Fe(CN)_6]^{3-/4-}$ from reaching the electrode surface due to the repulsive force between the negatively charged backbone of ss-DNA and the $[Fe(CN)_6]^{3-/4-}$ probe. A greater increase in the charge transfer resistance was observed for the ds-DNA modified GCE compared to that for the ss-DNA modified GCE. The formation of ds-DNA on the electrode surface greatly delayed the redox $[Fe(CN)_6]^{3-/4-}$ penetration to the GC active sites, and increased the interfacial electron-transfer resistance.

3.3. Effect of pH on the oxidation of quercetin

For studying the effect of pH on the oxidation signal of quercetin, the cyclic voltammograms of the solution containing Britton–Robinson buffer (0.1 M), KCl (0.1 M) and quercetin (250 μM) in different pH values were obtained. Fig. 7A shows the related cyclic voltammograms. According to this figure, the oxidation peak potential of quercetin was moved toward the more negative potentials with an increase of pH in the range of pH = (1–9). However, after pH = 9, no change was observed in the quercetin peak potential. Fig. 7B displays the alterations of the oxidation peak potential of quercetin in different pH values. As seen from Fig. 7B, between pH = 1 to pH = 7, the quercetin peak potential has been moved toward the more negative potentials with a Nernstian slope (0.06). After that, no change was observed. This proved that the numbers of transferred electrons and protons during the electrode reaction of quercetin are the same. Regarding the fact that quercetin and derivatives have pK_a values higher than 7,[31] under the condition of pH > pK_a, the electron exchange reaction was done without the proton transfer. Thus, no remarkable changes of the peak potentials were observed between pH (9 to 13). Fig. 7C shows the peak current alterations with pH too. According to Fig. 7C, the largest peak current is at the pH range of pH = 1 to 6. After that, the peak current is strongly reduced. As with Fig. 4A, at pH > 7, the oxidation peak of quercetin became wider, while its height was greatly reduced. So, considering the obtained

Table 2 Extracted EIS parameters of the bare GCE and ds-DNA modified GCE

Electrode	R_s (Ω)	CPE_P	CPE_T (Ω^{-1} cm^{-2} s^n)	R_{ct} (Ω cm^2)	W_R (Ω)
Bare GCE	427	0.97	1.48×10^{-5}	252	5358
ss-DNA/GCE	512	0.95	7.17×10^{-7}	5515	11 115
ds-DNA/GCE	535	0.95	8.38×10^{-7}	8492	18 526

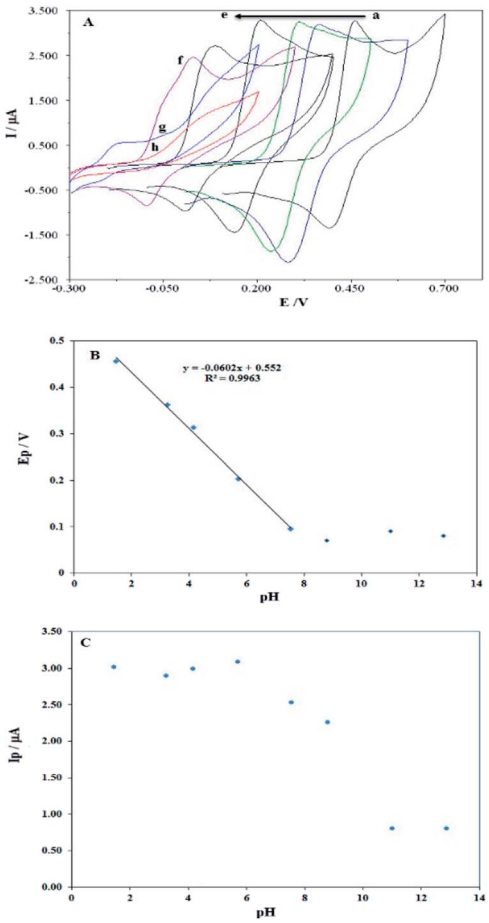

Fig. 7 Effect of pH on the oxidation signal of quercetin. Conditions: quercetin concentration: 250 μM, KCl: 0.1 M and Britton–Robinson buffer: 0.1 M.

results, the values between pH = 1 to pH = 6 can be chosen as a suitable pH range to record the cyclic voltammograms of quercetin.

3.4. Accumulation of quercetin

First, for studying the effect of the accumulation time, after polishing and washing, the electrode surface was modified by poly A, and then it was immersed in a solution of 0.35 M acetate buffer containing 83 mM NaCl and 16.7 μM quercetin in different time scales. DPV diagrams of each were then obtained.

In another part of this study, for finding an optimum quercetin concentration in the quercetin accumulation step, the poly A modified – GCE was placed in a solution containing different concentrations of quercetin.

Also, the diagram of the peak current changes in different concentrations are shown in Fig. 8B. It is clear that upon using concentrations of 30 μM and more, the accumulation of quercetin remains constant.

3.5. Probe immobilization conditions

Many factors affect the probe immobilization process. A number of these factors, such as time, applied potential and probe concentration, were investigated in this part.

3.5.1. Effect of the probe immobilization time. For studying the effect of time on the probe immobilization, GCE was immersed in the solution of probe (poly A). A potential of 0.5 V was then applied for 1–30 min. After accumulation of quercetin at the electrode surface, the DPV signal of the accumulated quercetin was measured. As resulted from Fig. 9A, the peak current of quercetin increases until 4 min. Then, in 4–10 min, it remains constant and subsequently reduces under longer times.

On the other hand, Fig. 9B shows the peak current of the adenine moiety of immobilized poly A at the electrode surface *versus* different probe immobilization times (as Fig. 8A shows the variations of the quercetin oxidation peak current in different accumulation times. It seems that after 10 min, the accumulation of quercetin at the electrode surface reaches its maximum. Increasing the time no longer affected the growth of the oxidation signal. This is probably due to the saturation of the electrode surface. As seen in Fig. 11, the adenine oxidation peak was observed at 1.18 V/SCE).

It should be noted that in order to decrease the time of accumulation, a higher concentration of quercetin (50 μM) was chosen. The effects of its accumulation time on DPVs were tested. So, because the DPV signals in the accumulation time of 5 min and concentration of 50 μM were nearly the same as the obtained time of 10 min and concentrations of 30 μM (results not shown), 5 min and 50 μM were chosen as the optimum accumulation time and quercetin concentration, respectively.

It is obvious that in the short time intervals of the probe immobilization, good arrangements of the probe molecules on the electrode surface make the quercetin accumulation more favourable. According to this figure, the peak current of adenine, which is related to immobilize poly A, confirms that the probe immobilization is remarkable in the first 5 min. The maximum peak current of quercetin is at a time span of 5 min.

Comparing the diagrams of A and B from Fig. 9, it is concluded that after 10 min, the peak current of the probe reaches its maximum. However, that of quercetin decreases. This is due to the reduction of its adsorption on the electrode surface as a result of the aggregation of the probe molecules. Therefore, 5 min was selected for the immobilization of the probe in subsequent studies.

3.5.2. Effect of the probe immobilization potential. The applied potential is one of the most important and effective parameters on the probe immobilization step. To do this, GCE was placed in a solution containing 5 μM poly A probe and different constant potentials between −0.5 to 0.5 V were applied. Then, after the accumulation of quercetin, DPVs were recorded. Fig. 10A shows the effect of the probe immobilization potential on the peak current of the accumulated quercetin.

Also, the effect of the probe immobilization potential on the peak current of adenine is shown in Fig. 10B. As seen from the figures, the probe immobilization at the negative potentials causes an increase in the quercetin accumulation on the DNA-modified electrode surface. So, the maximum peak current of quercetin is seen at −0.5 V. Similar results were achieved in our previous report[19] in the accumulation of methylene blue on the probe-modified pencil graphite electrode. There could be two reasons for this. One of the reasons is as follows: because of the

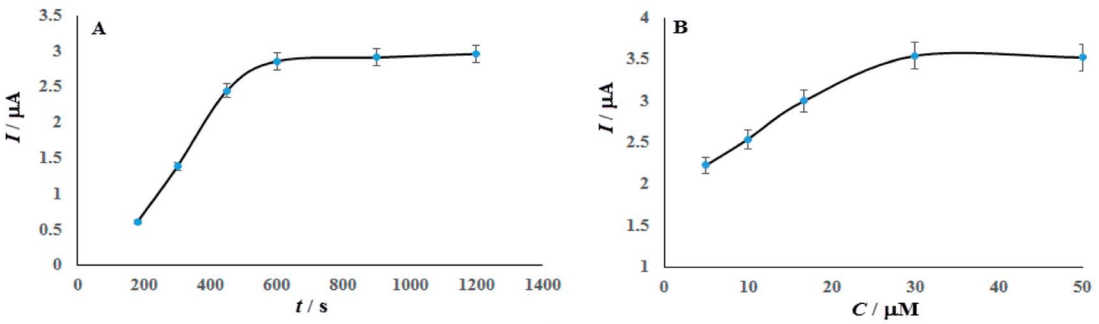

Fig. 8 (A) Effect of quercetin accumulation time on the DPV peak current of the accumulated quercetin using poly A modified – GCE. Experimental conditions: quercetin concentration: 16.7 μM, (B) Effect of quercetin concentration in the quercetin accumulation step on the DPV peak current of the accumulated quercetin using poly A modified – GCE. Experimental conditions: quercetin accumulation time: 10 min.

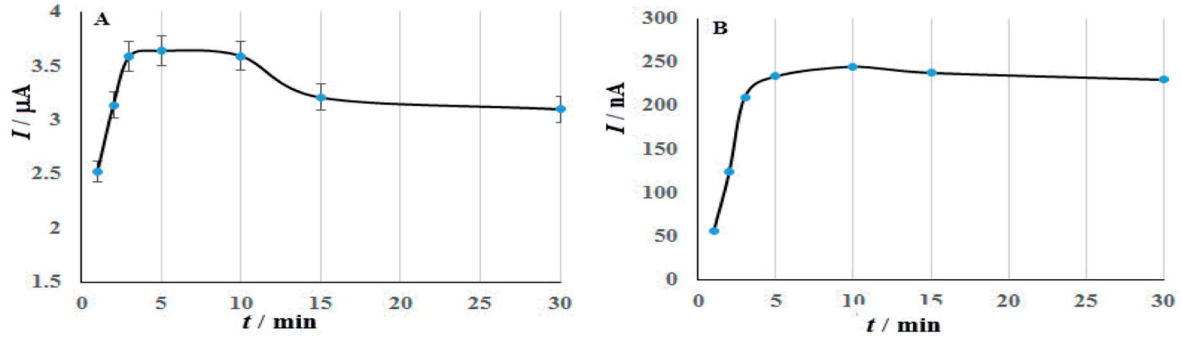

Fig. 9 Effect of the probe immobilization time on: DPV peak current of accumulated quercetin (A), and on DPV peak current of adenine of immobilized poly A oligonucleotide (B). Experimental condition: the accumulation of quercetin was conducted as described in Section 2.3.3 using 50 μM quercetin for 5 min. Concentration of poly A oligonucleotide: 5 μM.

electrostatic repulsion between the negative electrode surface and probe, fewer probes were immobilized at the electrode surface, so there would be more available sites for quercetin accumulation. However, as it is clear from Fig. 10B, at −0.5 V, the maximum amount of the probe was immobilized at the electrode surface. As a result, it can be said that the main mechanism for the immobilization of the probe on the GCE surface is not an electrostatic mechanism. As a result, −0.5 V was chosen for the immobilization of the probe in subsequent studies.

3.5.3. Effect of the probe concentration. In order to achieve the proper concentration of the probe, GCE was immersed into the solution of different amounts of the probe, (0.0–5.0) μM, and the potential of −0.5 V was applied for 300 s. After quercetin accumulation, DPV signals were obtained. Concentrations of the probe and the related peak currents of the accumulated quercetin are listed in Table 3. It is obvious that the quercetin peak current increased by probe concentration up to 3 μM and then remained constant. This is because of the saturation of the electrode surface with the DNA probe. Therefore, 3 μM was selected as the optimum probe concentration in the probe immobilization step.

3.5.4. Effect of the oligonucleotide type. To verify the effect of the immobilized polynucleotide type, as well as determining the type of possible interactions between quercetin and each of the nucleotides, the electrode surface was modified with various probes that consisted of similar nucleotides. For this purpose, four oligonucleotides, *i.e.*, poly A, poly T, poly C and poly G nucleotides, were utilized. The probe modified – GCE was placed into the solution containing quercetin. After its accumulation, their DPVs were recorded (Fig. 11). As seen in Fig. 11, an adenine oxidation peak was observed at 1.18 V/SCE. Peak current values corresponding to each probe are presented in Table 4. As seen in Fig. 11, the peaks of quercetin, guanine and adenine appeared at 0.24, 0.87 and 1.18 V, respectively. The peaks of guanine and adenine confirmed the immobilization of poly G and poly A, respectively, on the GCE surface. As seen in Table 4, similar accumulated quercetin peak currents were obtained using each of the probe modified – GCEs. Therefore, the accumulation of quercetin on the probe modified – GCE is a result of almost similar interaction between quercetin and each of the nucleotides. According to the literature review, most of the studies on the interaction of quercetin with DNA (which has been done inside the solution) declared that the interaction mechanism is intercalation.[16] Conversely, in our investigation, the proposed interactions that have taken place on the electrode surface cannot be intercalation. This is because, in our study, the signal decreased following hybridization. This is the indicative of the non-intercalation mechanism. According to our results, it is clear that quercetin has a stronger affinity toward ss-DNA than ds-DNA. For example, some studies show that the interaction between methylene blue and DNA is intercalation,

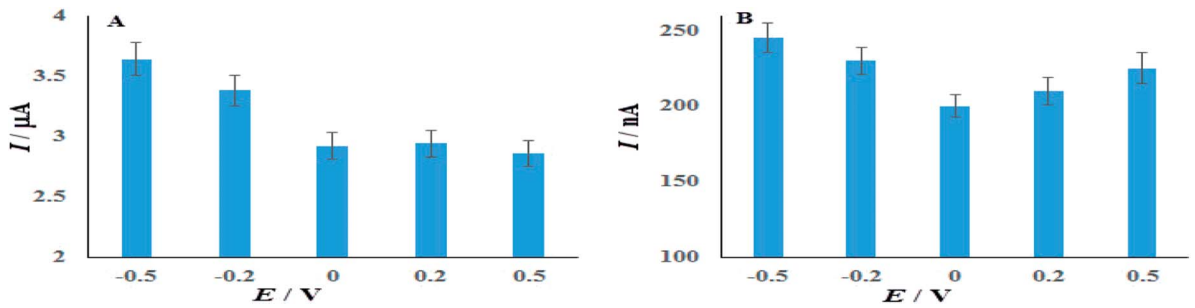

Fig. 10 (A) Histograms representing the variation of: peak current of accumulated quercetin (A), and peak current of adenine (B) *versus* different probe immobilization potentials. Experimental conditions as described in legend of Fig. 9. Probe immobilization time: 5 min.

Table 3 Effect of probe concentration on the quercetin peak current

Probe concentration (μM)	0	1	2	3	4	5
Peak current (μA)	2.34 ± 0.16	2.82 ± 0.18	3.24 ± 0.17	3.74 ± 0.18	3.68 ± 0.23	3.64 ± 0.19

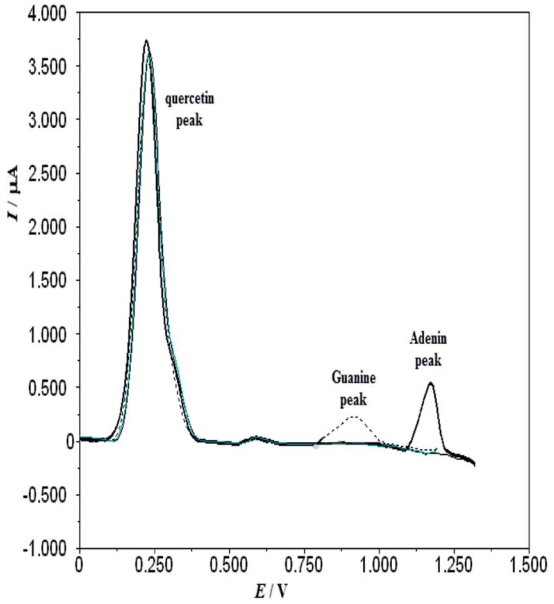

Fig. 11 DPVs obtained for various probe modified – GCE after quercetin accumulation. Experimental conditions are as described in the legend of Fig. 10. Probe immobilization potential: −0.5 V.

while some other studies explain that methylene blue has more affinity toward ss-DNA. The experimental conditions have a determinant effect on the interaction mechanism between DNA and small molecules. According to Table 4, due to the similar peak currents of the accumulated quercetin on the various poly nucleotide-modified GCE, it seems that there is no remarkable difference at the affinity of quercetin toward the four nucleotide types (adenine, guanine, cytosine and thymine). Also, it seems that maybe due to the formation of hydrogen bonds between quercetin (Fig. 12) and DNA bases, quercetin accumulated mostly on the ss-DNA modified electrode surface. However, because of the formation of the base pairs on the GCE electrode surface after hybridization, the hydrogen bonding interactions between quercetin and the bases are reduced.

3.6. Hybridization detection

In the following step, the hybridization effect was investigated. The poly A modified – GCE was immersed into the hybridization buffer solution (see Section 2.3.2), and the potential of 0.5 V was applied to the formation of an AT hybrid on the electrode surface. Then, the accumulation of quercetin was conducted at the obtained optimum experimental condition. Fig. 13 shows the DPVs of the accumulated quercetin for the poly A modified – GCE before (curve a) and after hybridization with the complementary oligonucleotide (poly T) (curve b). As seen in Fig. 13, the peak current of the accumulated quercetin was decreased, following the hybridization event. Similar results were observed in the hybridization between the poly G and poly C oligonucleotides. It seems that quercetin could not intercalate between ds-DNA. So, its interaction with the polynucleotides is not intercalation. Thus, the deduction is that quercetin probably has an interaction with the other parts of the DNA structure, which is the same among the polynucleotides, and also with the aromatic rings.

Thus, less quercetin could be accumulated on the electrode surface, resulting in the decrease of the peak current of accumulated quercetin on the electrode surface.

3.7. Selectivity study

An efficient DNA recognition biosensor should be sensitive just to the target DNA. In order to evaluate the selectivity of the designed DNA biosensor, the poly A modified – GCE was exposed to the non-complementary oligonucleotide (poly G). After the accumulation of quercetin, variations of the related peak currents were investigated. The DPVs of the poly A modified-GCE before (curve a) and after getting exposed to the poly G (curve b) are shown in Fig. 14.

As seen from curves a and b, there is not any remarkable difference between the signals of the accumulated quercetin at the electrode surface, showing that the hybridization between poly G and poly A did not occurred. The DPV of the poly A modified – GCE after exposure to the solution containing poly T is shown in Fig. 14 too (curve c). It is clear that because of the efficient hybridization, the peak current of quercetin at the electrode surface is decreased. Also, the DPV of poly A modified – GCE, which is the amount in the solution of poly G and poly T oligonucleotides, is shown in Fig. 14 (curve d). It can be seen that even at the presence of a non-complementary oligonucleotide (poly G) in solution, the poly T oligonucleotide could form a hybrid with the immobilized poly A at the GCE surface.

3.8. Evaluation of the performance of the biosensor

The influence of the complementary oligonucleotide concentration on the peak current of the accumulated quercetin was studied. The difference between the peak currents of the accumulated quercetin on the poly A modified – GCE in the absence

Table 4 Effect of the probe type on the quercetin peak current

Poly nucleotide type	Poly A	Poly T	Poly C	Poly G
Peak current (μA)	3.74 ± 0.18	3.61 ± 0.14	3.63 ± 0.19	3.52 ± 0.21

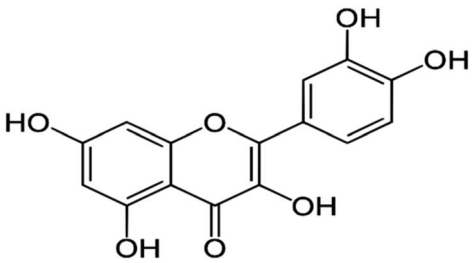

Fig. 12 Molecular structure of quercetin.

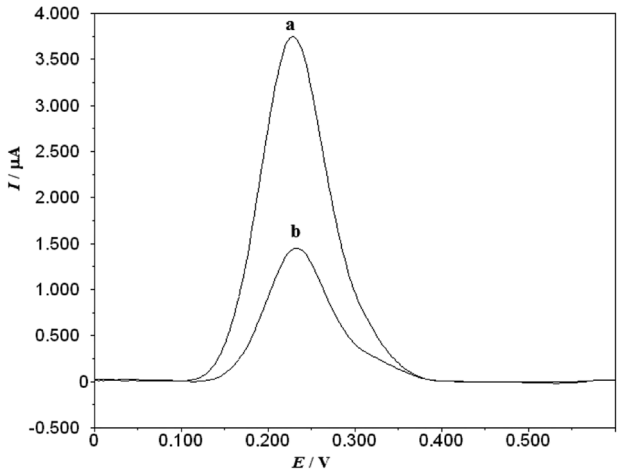

Fig. 13 DPVs of accumulated quercetin for the poly A modified – GCE before (a) and after hybridization with poly T (b). Experimental conditions as described in the legend of Fig. 11.

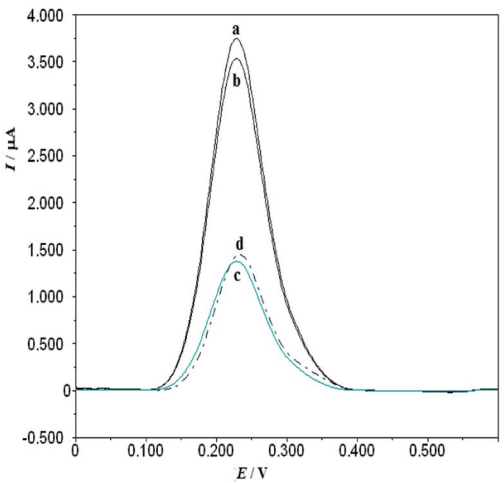

Fig. 14 DPVs of the accumulated quercetin for poly A modified – GCE before (a) and after interaction with: (b) poly G, (c) poly T, and (d) mixture of poly G and poly T. Experimental conditions as described in the legend of Fig. 11.

and presence of various concentrations of complementary oligonucleotide (poly T) were calculated. Fig. 15 presents the DPVs of the poly A modified – GCE before (curve a) and after

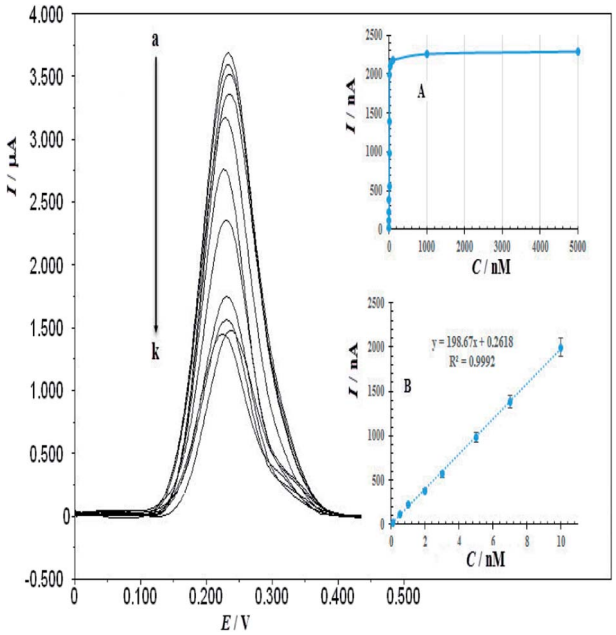

Fig. 15 DPVs of accumulated quercetin on the poly A modified – GCE after hybridization with poly T target oligonucleotide with different concentrations: (a) 0, (b) 0.1, (c) 1, (d) 2, (e) 3, (f) 5, (g) 7, (h) 10, (i) 100, (j) 1000, (k) 5000 nM. Inset showing the variation of the difference between the peak currents of quercetin on the poly A modified – GCE in the presence and absence of the poly T target sample (Δ*I*) *versus* target concentration in the range of (A) 0.1–5000 nM and (B) 0.1 to 10 nM. Experimental conditions as described in the legend of Fig. 11.

hybridization with various concentrations of poly T oligonucleotide (curves b–k). The ΔI changes ($\Delta I = I_{\mathrm{p\ probe}} - I_{\mathrm{p,hyb}}$) *versus* the concentrations of poly T are shown in insets A and B of Fig. 15.

As seen from Fig. 15, ΔI increases with the concentration of poly T up to 0.1 μM. So, it is concluded that in the 0.1 μM concentration of the poly T oligonucleotide, almost all of the probe molecules take part in hybridization. As a result, the increase of the complementary oligonucleotide concentration does not have any remarkable effect on ΔI increasing. So, according to Fig. 15, the prepared biosensor has a linear range between 0.1–10.0 nM for the complementary oligonucleotide, and the obtained limit of detection is 83 pM. The relative standard deviation over three independent probe-modified electrodes measured at 5 nM HCV1a was 4.7%, indicating a remarkable reproducibility of the detection method.

3.9. Detection of the short sequences of the hepatitis C virus using quercetin

Fig. 16 displays the DP voltammograms for the accumulated quercetin at the PHCV1 probe-modified GCE before (curve a) and after hybridization with the complementary HCV1a oligonucleotide (curve b). As seen in Fig. 16, the highest signals are observed for the PHCV1 probe-modified GCE before hybridization with the complementary HCV1a oligonucleotide (curve a). The peak current of the accumulated quercetin was decreased, following the hybridization event. This indicated that quercetin

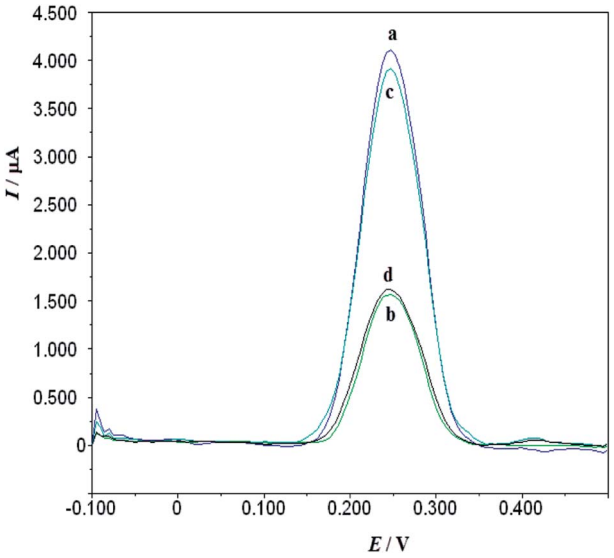

Fig. 16 DPVs of accumulated quercetin at the PHCV1 probe-modified GCE: (a) before, (b) after hybridization with the complementary HCV1a oligonucleotide, (c) after interaction with the non-complementary HCV3a target, and (d) after hybridization with a mixture of both complementary HCV1a and non-complementary HCV3a sequences. Oligonucleotide concentrations were 5 μM. Other experimental conditions were as described in the legend of Fig. 11.

could not intercalate between ds-DNA. It is concluded that the decrease in the quercetin signal represents the extent of the hybridization at the electrode surface. Having observed the ability of the electrode in detecting the target complementary HCV1a oligonucleotide, an investigation concerning the interaction of the probe with a non-complementary HCV3a oligonucleotide was conducted. Fig. 16 displays the DP voltammogram for the accumulated quercetin at the PHCV1 probe-modified GCE after interaction with the non-complementary HCV3a target (curve c). The results indicated that no remarkable interaction between the HCV3a oligonucleotide and PHCV1 probe-modified GCE exists. The selectivity of the biosensor was also accomplished in the samples containing both complementary and non-complementary sequences. For this purpose, the PHCV1 probe was immobilized on the GCE surface, and then the solution containing both complementary and non-complementary sequences (mixture of 5 μM HCV1a and 5 μM HCV3a) was used for hybridization (Fig. 16, curve d). As seen in Fig. 16 (curve d), the presence of HCV3a in the mixed solution has a negligible effect on the hybridization between the immobilized probes and the complementary oligonucleotide. Thus, the biosensor can detect fully matched complementary targets in a mixed solution of complementary and non-complementary oligonucleotides, and the high selectivity of this strategy was confirmed.

4. Conclusion

In order to introduce the quercetin as a new electroactive indicator for DNA hybridization detection, an electrochemical DNA biosensor was prepared based on immobilizing an oligonucleotide as a DNA probe at the electrode surface. The hybridization of the probe with the complementary oligonucleotide took place subsequently. After accumulation of quercetin on the probe modified – GCE before and after hybridization with the target sample, the related DPVs were obtained. Then, the optimized conditions for better performance of biosensor were achieved. Quercetin is better accumulated on the probe modified – GCE. After hybridization, peak currents of the accumulated quercetin are decreased. Also, there are no specific differences between the interactions of quercetin with various types of nucleotides. The difference between the peak currents of the accumulated quercetin before and after DNA hybridization makes the probe modified GCE a useful tool for further developments of an indicator – based biosensor for the detection of DNA hybridization events. The developed biosensor was applied successively for the detection of short sequences of hepatitis C virus (HCV1). Although the proposed biosensor has the ability to detect some DNA-based disease biomarkers, it should be noted that due to the very low concentrations of biomarkers in real biological samples, developing the more sensitive and reliable biosensors for the early detection of dangerous disease biomarkers needs a much lower limit of detection, and the related research studies are in progress in our laboratory.

Conflicts of interest

There are no conflicts to declare.

References

1 F. Lucarelli, G. Marrazza, A. P. Turner and M. Mascini, *Biosens. Bioelectron.*, 2004, **19**, 515–530.
2 K. J. Odenthal and J. J. Gooding, *Analyst*, 2007, **132**, 603–610.
3 E. Paleček, M. Fojta, M. Tomschik and J. Wang, *Biosens. Bioelectron.*, 1998, **13**, 621–628.
4 J. Justin Gooding, *Electroanalysis*, 2002, **14**, 1149–1156.
5 J. Tosar, G. Branas and J. Laíz, *Biosens. Bioelectron.*, 2010, **26**, 1205–1217.
6 J. Wang, G. Rivas, J. R. Fernandes, J. L. L. Paz, M. Jiang and R. Waymire, *Anal. Chim. Acta*, 1998, **375**, 197–203.
7 M. H. Pournaghi-Azar, M. S. Hejazi and E. Alipour, *Electroanalysis*, 2007, **19**, 466–472.
8 C. Fan, K. W. Plaxco and A. J. Heeger, *Proc. Natl. Acad. Sci. U. S. A.*, 2003, **100**, 9134–9137.
9 M. S. Hejazi, M. H. Pournaghi-Azar, E. Alipour, E. D. Abdolahinia, S. Arami and H. Navvah, *Electroanalysis*, 2011, **23**, 503–511.
10 M. Pournaghi-Azar, F. Ahour and M. Hejazi, *Anal. Bioanal. Chem.*, 2010, **397**, 3581–3587.
11 M. H. Pournaghi-Azar, E. Alipour, S. Zununi, H. Froohandeh and M. S. Hejazi, *Biosens. Bioelectron.*, 2008, **24**, 524–530.
12 Y. Temerk, M. Ibrahim, H. Ibrahim and W. Schuhmann, *RSC Adv.*, 2018, **8**, 25387–25395.
13 Y. Temerk and H. Ibrahim, *J. Electroanal. Chem.*, 2015, **736**, 1–7.

14 Y. Temerk and H. Ibrahim, *J. Pharm. Biomed. Anal.*, 2014, **95**, 26–33.
15 M. Ibrahim, H. Ibrahim, N. B. Almandil, M. A. Sayed, A. N. Kawde and Y. Aldaqdouq, *Electroanalysis*, 2020, **32**, 2146–2155.
16 M. Ibrahim, H. Ibrahim, N. B. Almandil, M. A. Sayed and A.-N. Kawde, *Anal. Methods*, 2020, **12**, 2846–2857.
17 A. Erdem, B. Meric, K. Kerman, T. Dalbasti and M. Ozsoz, *Electroanalysis*, 1999, **11**, 1372–1376.
18 W. Yang, M. Ozsoz, D. B. Hibbert and J. J. Gooding, *Electroanalysis*, 2002, **14**, 1299–1302.
19 M. H. Pournaghi-Azar, M. S. Hejazi and E. Alipour, *Anal. Chim. Acta*, 2006, **570**, 144–150.
20 H.-W. Gao, P. Qin, C. Lin, Z.-M. Shang and W. Sun, *J. Iran. Chem. Soc.*, 2010, **7**, 119–127.
21 H. Cai, X. Cao, Y. Jiang, P. He and Y. Fang, *Anal. Bioanal. Chem.*, 2003, **375**, 287–293.
22 H. Cai, Y. Wang, P. He and Y. Fang, *Anal. Chim. Acta*, 2002, **469**, 165–172.
23 K. Maruyama, J. Motonaka, Y. Mishima, Y. Matsuzaki, I. Nakabayashi and Y. Nakabayashi, *Sens. Actuators, B*, 2001, **76**, 215–219.
24 M. e. H. Pournaghi-Azar, F. Ahour and M. e. S. Hejazi, *Electroanalysis*, 2009, **21**, 1822–1828.
25 N. Zhu, A. Zhang, Q. Wang, P. He and Y. Fang, *Anal. Chim. Acta*, 2004, **510**, 163–168.
26 J. Kang, L. Zhuo, X. Lu, H. Liu, M. Zhang and H. Wu, *J. Inorg. Biochem.*, 2004, **98**, 79–86.
27 J. Labuda, M. Bučková, Ľ. Heilerová, S. Šilhár and I. Štepánek, *Anal. Bioanal. Chem.*, 2003, **376**, 168–173.
28 A. M. Oliveira-Brett and V. C. Diculescu, *Bioelectrochemistry*, 2004, **64**, 143–150.
29 Z. Zhu, C. Li and N.-Q. Li, *Microchem. J.*, 2002, **71**, 57–63.
30 R. S. Nicholson, *Anal. Chem.*, 1965, **37**, 1351–1355.
31 M. Dueñas, F. Surco-Laos, S. González-Manzano, A. M. González-Paramás and C. Santos-Buelga, *Eur. Food Res. Technol.*, 2011, **232**, 103–111.